Many-body polarization and overlap effects in the dynamic structure factor of dense krypton gas

J. J. Salacuse
Science and Mathematics Department, GMI Engineering and Management Institute, 1700 West Third Avenue, Flint, Michigan 48502-2276

W. Schommers
Institut für Nucleare Festkörperphysik, Kernforschungszentrum Karlsruhe, D-7500 Karlsruhe, West Germany

P. A. Egelstaff
Department of Physics, University of Guelph, Guelph, Ontario, Canada N1G 2W1
(Received 5 December 1985)

Molecular-dynamics computer simulations of dense krypton gas have been carried out for $\rho = 13.8$ atoms/nm^3 and $T = 297$ K, with use of the best available pair potentials. The results are compared to published experimental data at this state to discover the role of the many-body potentials of the atoms on their dynamics. It is found that these effects produce a marked slowing down of many-body collision processes.

I. INTRODUCTION

This is the second in a series of investigations[1] in which the results of molecular-dynamics (MD) simulations, based on pair theory and using the best available pair potentials for krypton, are compared to experimental krypton data.[2] Specifically, the dynamic structure factors obtained from simulations using the pair potentials of Aziz[3] and Barker *et al.*[4] are compared to the experimentally-determined dynamic-structure factor.[2] This comparison is made for dense krypton gas at a temperature of 297 K and a density of 13.84×10^{27} atoms/m^3, which is about twice the critical density.

The conventional pair theory of atomic fluids assumes that once the pair potential is known, the atoms may be represented as rigid particles interacting with this pair potential. If the latter represents the real interaction between two atoms it includes the usual nonrigidity effects such as polarization, overlap, etc. Therefore, the approximation inherent in the pair theory, is that these effects will be considered at the level of two-body interactions but neglected at three-body or higher levels. We are investigating how large an error this introduces in calculations of the dynamics at the atomic level. Therefore, we try to make our computer simulation the best estimate of the exact pair theory prediction.

A qualitatively consistent and quantitatively significant difference in simulation and experimental results is found in the momentum transfer ($\hbar q$) range, $0.60\ \text{Å}^{-1} \leq q \leq 1.30\ \text{Å}^{-1}$. The experimental dynamic-structure factor has a higher peak and is narrower than that determined from the simulations. This effect initially appears at q of 1.30 Å^{-1} and increases as q is decreased to the minimum value accessible in the simulations of 0.60 Å^{-1}. There is agreement at high q. In our earlier study, a qualitatively similar difference in experimental and simulation results were observed at a q of 0.80 Å^{-1}. In the present case the density is about 30% larger which seemingly accounts for the more significant difference in these results.

The pair potentials of Aziz[3] and Barker *et al.*[4] closely agree with one another. Their correctness is suggested, indirectly, by the fact that both yield gas-phase properties that agree nicely with experimental data. Recently, Barocchi *et al.*[5] obtained a pair potential for krypton from experimental structure data at low densities, and compared this to the Barker *et al.*[4] potential thus providing a direct test. Excellent agreement was found except for a small discrepancy in the range 5–10 Å.

The above comments suggest the pair potentials used in the simulations closely agree with the true pair potential for krypton. Hence, it is unlikely that the differences we observe in the simulated and experimental dynamic-structure factors result from the form of the pair potential used in the simulations. We feel that these differences are a result of a failure in the pair theory; that is, the neglect of effects such as polarizability and overlap in the many-body terms and so are not accounted for in the simulation. These effects would involve three or more atoms and so involve distance ranges corresponding to $q \sim 1$ Å^{-1}.

There has been considerable discussion about the magnitude and role of many-body forces in atomic fluids. For example, in a review, Barker[6] expresses the view that "many-body interactions other than the triple-dipole Axilrod-Teller interaction are relatively unimportant." Barker notes that pair plus Axilrod-Teller interactions nicely describe pressure-volume-temperature as the third virial coefficient of argon. However, in regard to the importance of many-body forces with respect to the structure of dense krypton gas, Egelstaff and co-workers have shown that the Axilrod-Teller interaction is relatively unimportant while non Axilrod-Teller interactions are significant in determining the static structure factor $S(q)$ at high densities for q in the range 0.3–1.0 Å^{-1}. Teitsma

 ©1986 The American Physical Society

and Egelstaff[7] demonstrated that the Axilrod-Teller interaction did not adequately describe the third virial coefficient of $S(q)$. Egelstaff, Teitsma and Wang,[8] and Egelstaff *et al.*[2] showed that the Axilrod-Teller term does not generate the correct density dependence to explain the observed behavior of $S(q)$ for krypton. More detailed experimental studies are required to resolve the problems evident in this field, and for this reason we have (in our earlier paper and here) tried to extend these investigations to the most sensitive data available, namely that for the dynamic-structure factor. Papers by Schommers[9,10] reporting MD simulations of the velocity correlation function and other dynamic properties, indicate that these data are likely to be more sensitive to many-body terms than even the static structure factor. Moreover, the sensitivity is enhanced by the comparison of experimental data with good computer simulations using reliable pair potentials for real krypton atoms. Thus our objective is much wider than an examination of rival claims about particular forces. We would like to understand the physical properties that are influenced the most by many-body forces.

The simulated dynamic structure factor is determined from a pair of independent MD simulations. In Sec. II the simulation procedures are discussed. In Sec. III a comparison of the MD results is given, discrepancies between these results are noted and reasons for these discrepancies are suggested. A comparison of simulation and experimental results is given in Sec. IV. In that section, we report the difference between experimental and simulation results for $q \leq 1.30$ Å^{-1} and our interpretation of this. We also comment on the consequences of differences in the experimental and simulated dynamic-structure factor on the fluid structure and many-body collision processes. Conclusions and suggestions for future work are given in Sec. V.

II. MOLECULAR-DYNAMICS CALCULATIONS

The microscopic number density for a system of N particles with positions $\mathbf{r}_j(t), j=1,2,\ldots,N$, is defined as

$$\rho(\mathbf{r},t)=\sum_j \delta(\mathbf{r}-\mathbf{r}_j(t)) . \tag{1}$$

Taking the Fourier transform of $\rho(\mathbf{r},t)$ gives

$$\rho_{\mathbf{q}}(t)=\sum_j \exp[i\mathbf{q}\cdot\mathbf{r}_j(t)] . \tag{2}$$

The intermediate scattering function, $I(\mathbf{q},t)$, is defined as the self-correlation of $\rho_{\mathbf{q}}(t)$, thus

$$I(\mathbf{q},t)=\frac{1}{N}\langle \rho_{-\mathbf{q}}(0)\rho_{\mathbf{q}}(t)\rangle = \frac{1}{N}\left\langle \sum_{j,k} \exp\{i\mathbf{q}\cdot[\mathbf{r}_j(t)-\mathbf{r}_k(0)]\}\right\rangle , \tag{3}$$

where $\langle\ \rangle$ represents the equilibrium ensemble average. $I(\mathbf{q},t)$ is related to the dynamic-structure factor (also called the scattering function), $S(\mathbf{q},\omega)$, by

$$S(\mathbf{q},\omega)=\frac{1}{2\pi}\int_{-\infty}^{+\infty} dt \exp(i\omega t) I(\mathbf{q},t) . \tag{4}$$

$I(\mathbf{q},t)$ is related to the van Hove correlation function $G(\mathbf{r},t)$ by

$$I(\mathbf{q},t)=\int d\mathbf{r}\exp(i\mathbf{q}\cdot\mathbf{r})G(\mathbf{r},t) . \tag{5}$$

The quantity $G(\mathbf{r},t)d\mathbf{r}$ gives the probability of finding a particle within an element $d\mathbf{r}$ at $\mathbf{r}$ at time t given there was an arbitrary reference particle at $\mathbf{r}=\mathbf{0}$, at time $t=0$. Hence, $G(\mathbf{r},t)$ describes the structure of a fluid in both space and time. In this sense equations (4) and (5) relate $S(\mathbf{q},\omega)$ and $I(\mathbf{q},t)$ to the fluid structure. We are concerned with an isotropic fluid which implies that S and I depend upon $\mathbf{q}$ through its magnitude q, and G is a function of $\mathbf{r}$ through its magnitude r.

The simulation procedure requires the use of periodic boundary conditions which produce a spatial periodicity in the structure of the simulated fluid and hence in $G(\mathbf{r},t)$. This periodicity restricts the nonzero $\mathbf{q}$ values to

$$\mathbf{q}=\frac{2\pi}{L}(l_1,l_2,l_3) , \tag{6}$$

where L is the box length used in the simulation and $l_i=0,\pm1,\pm2,\ldots$, with $i=1,2$. For a given wave vector $\mathbf{q}$, $I(\mathbf{q},t)$ can be obtained via equation (3) with the particle positions $\mathbf{r}_i(t)$ determined from the simulation and the ensemble average calculated as a time average. $I(q,t)$ is obtained as an average over all $I(\mathbf{q},t)$ for which $\mathbf{q}$ is consistent with restriction (6) and has magnitude in the range $[q,q+dq]$. Alternately, one can obtain an expression for $I(q,t)$ by averaging equation (3) over all $\mathbf{q}$ values of magnitude of q. This gives

$$I(q,t)=\frac{1}{N}\left\langle \sum_{j,k} \frac{\sin[qr_{jk}(t)]}{qr_{jk}(t)}\right\rangle , \tag{7}$$

where

$$r_{jk}(t)=|\,\mathbf{r}_j(t)-\mathbf{r}_k(0)\,| .$$

The $r_{jk}(t)$ are obtained from the simulation and processed according to equation (7) with the ensemble average calculated as a time average to give $I(q,t)$ directly. We have obtained $I(q,t)$ by both of the methods described above.

The error associated with the simulation of $I(q,t)$ generally increases with decreasing q for a given box size L. As q decreases the number of $\mathbf{q}$ values consistent with restriction (6) decreases giving a smaller sample from which to estimate $I(q,t)$ and thus giving a less accurate estimate. As seen by equation (6) the situation is improved by increasing L. Also as q decreases the t value beyond which $I(q,t)$ can be assumed zero generally increases and this implies a longer time interval over which the fluid must be simulated. However, $I(q,t)$ can be accurately simulated only over time intervals less than the time required for a density fluctuation (sound wave) to travel the box length L. Simulating over longer time intervals will produce errors in $I(q,t)$ which arise from the spurious reappearance of the sound wave as a result of the periodic boundary conditions. Thus for a given L, decreasing q will eventually produce errors in $I(q,t)$ of the above type. Again the situation is improved by increasing L. The relationship of the error in $I(q,t)$ and the box size L can be checked roughly in our work since we have performed a pair of in-

dependent simulations with distinct L values from which $I(q,t)$ is obtained.

Series I calculations were performed at the University of Guelph on a Floating Point Systems Array Processor, model FPS-164, with an IBM 3081D used as a host machine. The MD simulation was carried out for 256 particles interacting via an Aziz[3] pair potential with diameter σ and well depth ϵ/k of 3.579 Å and 200 K, respectively, and a cut-off radius of 2.5σ. The fluid was simulated in a cubical box of length $L=26.6$ Å with periodic boundary conditions. The particle positions resulting from the simulation were processed via equation (7) to give $I(q,t)$ for q values of 0.6, 0.80, 1.05, 1.30, 1.55, 1.80, 2.10, 2.40, 2.70, 3.00, 3.25, and 3.50 Å^{-1}.

Series II calculations were performed at KFA, Karlsruhe on an IBM 3033. In this case 500 particles interacting according to the pair potential of Barker *et al.*[4] with a σ of 3.61 Å and ϵ/k of 199 K (with a cut-off radius of 3.6σ) were simulated in a cubical box of length $L=33.1$ Å with periodic boundary conditions. $I(\mathbf{q},t)$ values were obtained by use of equation (3) and these values were then averaged to give $I(q,t)$ as previously described. The same series of q values were used.

The pair potentials of Aziz[3] and Barker *et al.*[4] are in good agreement. Hence any differences in series I and II estimates of $I(q,t)$ are not expected to result from the use of different forms of the krypton potential. Series I and II estimates of $I(q,t)$ were extended to t values for which the magnitude of $I(q,t)$ was of the order 10^{-3}. The $I(q,t)$ were assumed to be zero for larger values of t and were numerically transformed according to equation (4) to give $S(q,\omega)$.

Experimental results are in the form $S(q,\omega)_* R(\omega)$ where the asterisk represents the convolution operation and $R(\omega)$ is a resolution function which is well approximated by a Gaussian in ω. Use of the convolution theorem and equation (4) show the transform of $S(q,\omega)_* R(\omega)$ to be $I(q,t)R(t)$ where $R(t)$ is the transform of $R(\omega)$ and has form $^1\exp(-t^2/6.6)$ with t in units of 10^{-12} sec. In order to compare experimental and simulated results, the simulated estimates of $I(q,t)$ are multiplied by $R(t)$ and transformed to give $S(q,\omega)_* R(\omega)$.

III. COMPARISON OF MD RESULTS

The results of series I and II calculations and the agreement between these results is illustrated in Figs. 1 and 2. The original $I(q,t)$ estimates from both series are compared in Fig. 1 for q values 0.80, 1.80, 2.40, and 3.00 Å^{-1}. It can be seen that in some instances there are discrepancies in peak height or in the long-time behavior. These will be discussed further below, where we shall argue that they are likely due to inadequate phase-space averaging.

The quantity $I(q,t)R(T)/S(q)$ is plotted against t in Fig. 2 for a representative set of q values. As previously noted, the factor $R(t)$ is included to allow direct comparison to experimental results. The normalization constant $S(q)=I(q,0)$ is included so as to best describe the manner in which the correlation function $I(q,t)$ damps to zero in time. As seen in Fig. 2, for a given q-value series I and II results agree quite well for small values of t with moderate differences appearing in the range 0.5×10^{-12} sec to 10^{-12} sec. Larger discrepancies occur for $t>10^{-12}$ sec at the lower q values for which the $I(q,t)$ remain nonzero over a longer time interval. The curves associated with q values of 1.80 and 0.60 Å^{-1} are particularly worth noting. For $q=1.80$ Å^{-1} the disagreements between series I and II results are relatively large and occur at small values of time when compared to other q value results. Also note the large discrepancies in the $q=0.60$ Å^{-1} case in addition to the lack of smoothness in the individual curves, especially the series I curve.

The simulations which produced series I and II results differed in the averaging technique used to obtain $I(q,t)$, the box size L, and the set of initial conditions used to generate an iterative solution of the equations of motion. Each of these distinctions has the possibility of producing

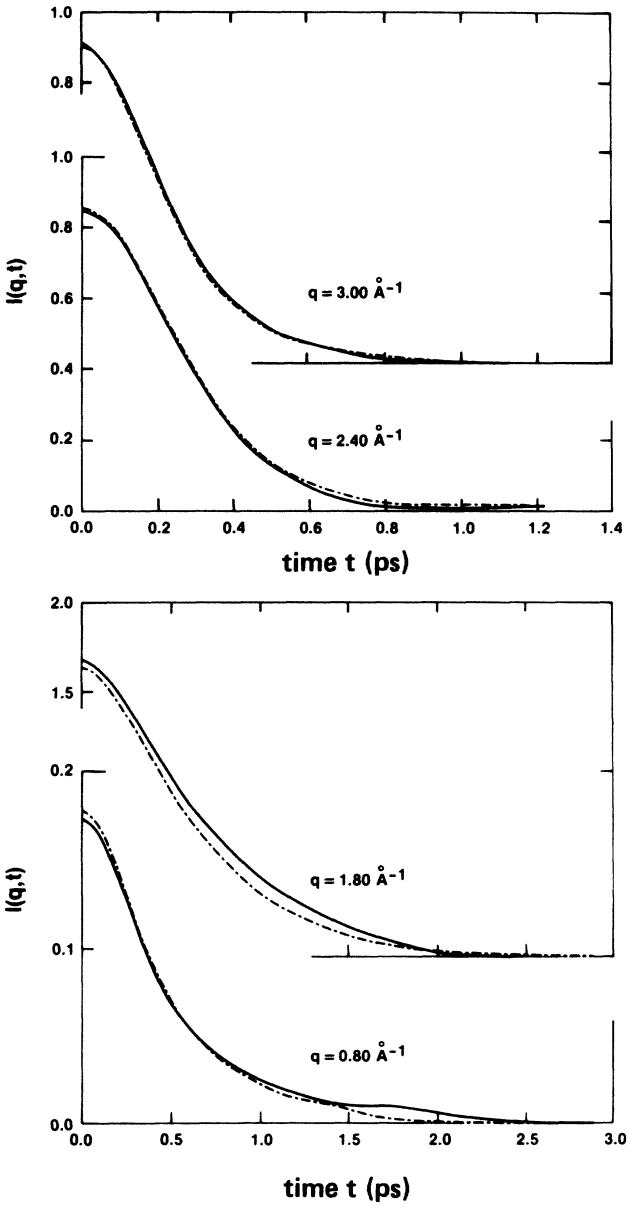

FIG. 1. Examples of the original $I(q,t)$ for series I and II.

differences in the $I(q,t)$ estimates. The excellent agreement for the $q=2.40$ Å^{-1} case indicates the averaging techniques are not affecting the results. The finite box size is a source of error which becomes more significant for small q values and is likely affecting the $q=0.60$ Å^{-1} results as suggested by the lack of smoothness of the curve for series I in this case. As q increases there is no significant difference in smoothness of the individual curves associated with a particular q value, nor is there a consistent manner in which the curves differ from one another as q is varied. Thus it is unlikely the box size is appreciably affecting the series I and II results for the larger q values.

The simulation procedure can be viewed as following, or more correctly generating, a path of the system in phase space, sampling particle positions along this path by storing the $\mathbf{r}_i(t)$ every, say, ten iterations and using these values to obtain an estimate of $I(q,t)$. The series I and II calculations use different initial particle positions and hence follow distinct phase paths. Estimates of $I(q,t)$ obtained as time averages over different phase paths should closely agree if the individual paths adequately sample phase space. An inadequate sampling of phase space will produce discrepancies in the $I(q,t)$ estimates and this is likely the cause of the differences in the series I and II curves at large-t values. Matters should improve by extending the lengths of the MD simulations from which the $I(q,t)$ estimates are obtained or by averaging results.[11]

As a final point in the discussion of the results shown in Fig. 2, consider the $q=1.80$ Å^{-1} case which produced the largest $S(q)$ value and the broadest $I(q,t)$. The value of 1.80 Å^{-1} closely approximates $2\pi/d$, with d being the average distance between particles in contact. There is a maximum in $S(q)$ at $q=1.80$ Å^{-1}, which produces a

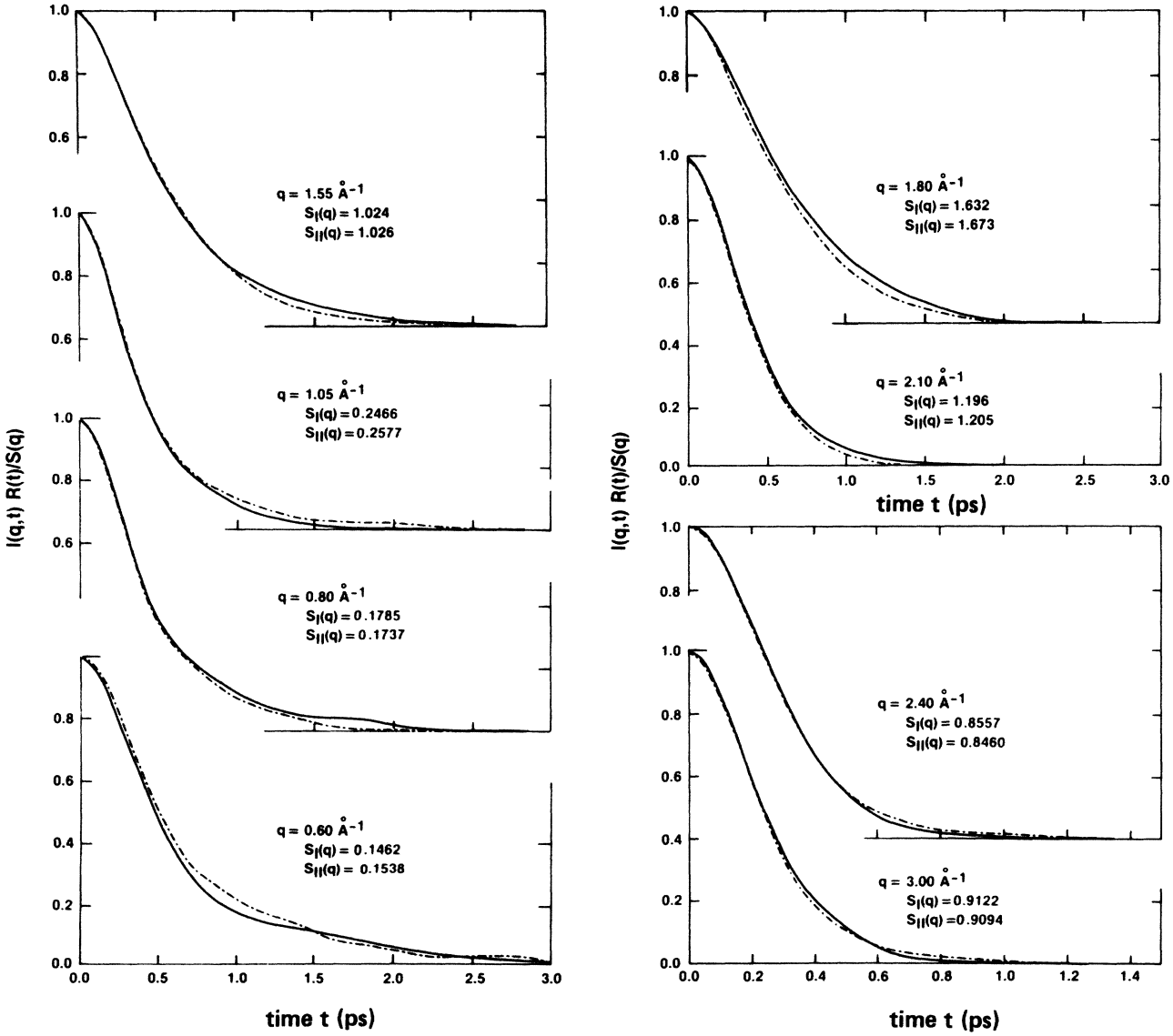

FIG. 2. $I(q,t)R(t)/S(q)$ vs t for fixed q with $S(q)=I(q,0)$. The dotted line represents series I results and the solid line represents series II results. $S_{\mathrm{I}}(q)$ and $S_{\mathrm{II}}(q)$ are series I and II values of $S(q)$.

narrow $S(q,\omega)$ vs ω curve, referred to as DeGennes narrowing.[12] This in turn produces a broad $I(q,t)$ vs t curve. The relatively large difference in series I and II results in this case most likely suggests the need for more extensive sampling of phase space for this case. A possible explanation is that the fluid structure which gives rise to the $q=1.80$ Å^{-1} Fourier component of $G(r,t)$, can decay slowly in a variety of ways thus requiring extensive phase-space sampling to yield accurate estimates of $I(q,t)$.

Figure 3 shows plots of $S(q,\omega)_* R(\omega)$ vs ω for fixed q values. The Fourier transform of $I(q,t)R(t)$ is $S(q,\omega)_* R(\omega)$; hence, the curves of Figs. 2 and 3 are transform pairs apart from the factor $S(q)$. The curves of Fig. 3 are unnormalized and thus represent an absolute measure of the agreement between series I and II results. However, for a given q value the agreement between these curves is fairly predictable from the analogous curves of Fig. 2. For example, the Figs. 2 and 3 curves for $q=2.40$ Å^{-1} agree quite well, while the $q=1.80$ Å^{-1} results show a relatively large disagreement. Also note the oscillatory nature of the $q=0.60$ Å^{-1} curves in Fig. 3 which result from the poor quality of the analogous curves of Fig. 2.

IV. COMPARISON OF SIMULATION AND EXPERIMENTAL RESULTS

Figure 4 shows a comparison between experimental and simulation results. The quantity $S(\omega)_* R(\omega)$ vs ω is plotted for a given q value. The experimental results of Ref. 2 had been interpolated to a table of data for each of the q's required by Glasser and Egelstaff.[13] The dots give the experimental results; the solid line represents an equally weighted average of series I and II calculations. For q values of 1.55, 1.80, and 2.10 Å^{-1} the agreement between experiment and simulation is quite good. For example, in the case of $q=1.80$ Å^{-1} the maximum difference be-

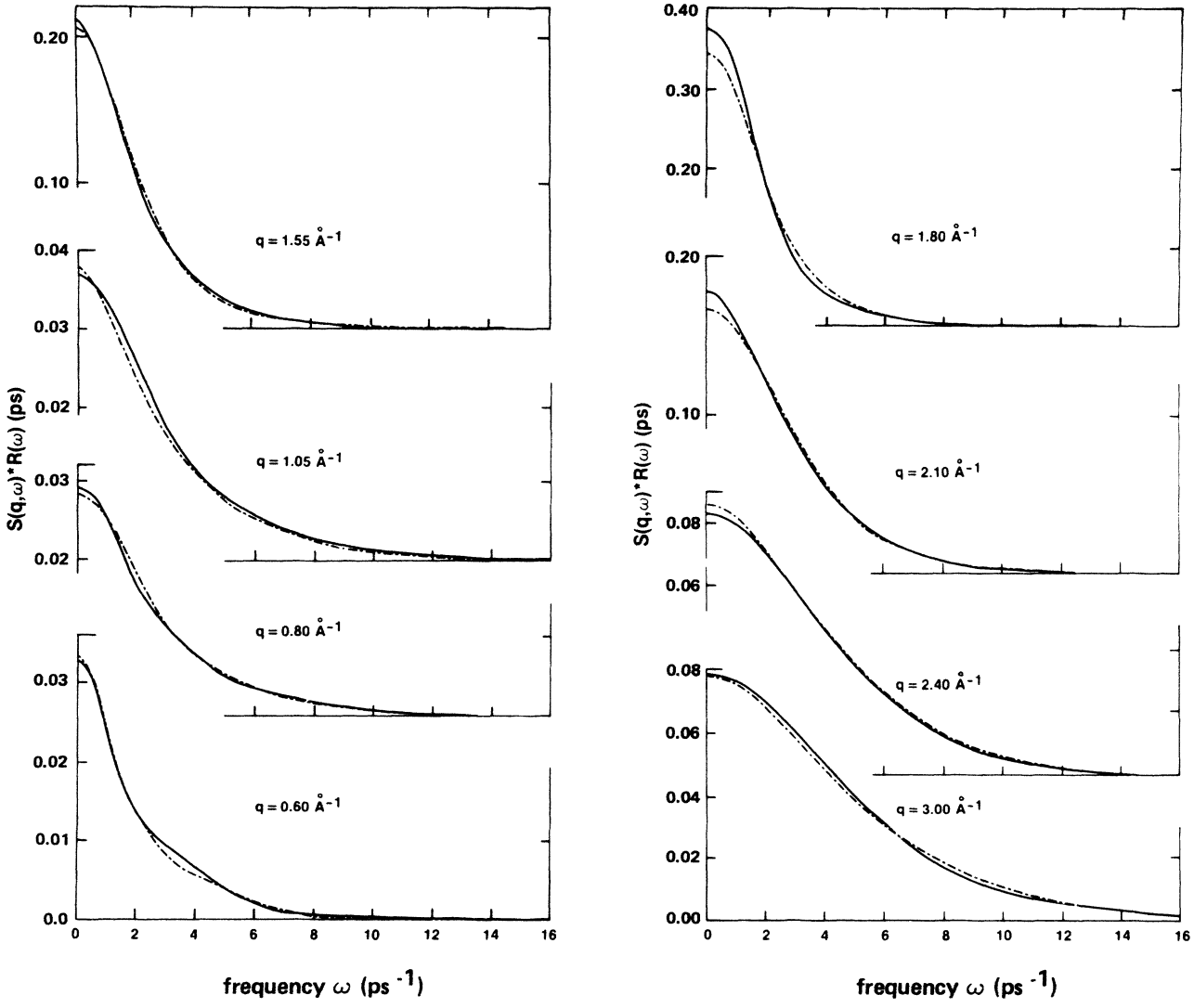

FIG. 3. $S(q,\omega)_* R(\omega)$ vs ω for fixed q. The dotted line represents series I results and the solid line represents series II results.

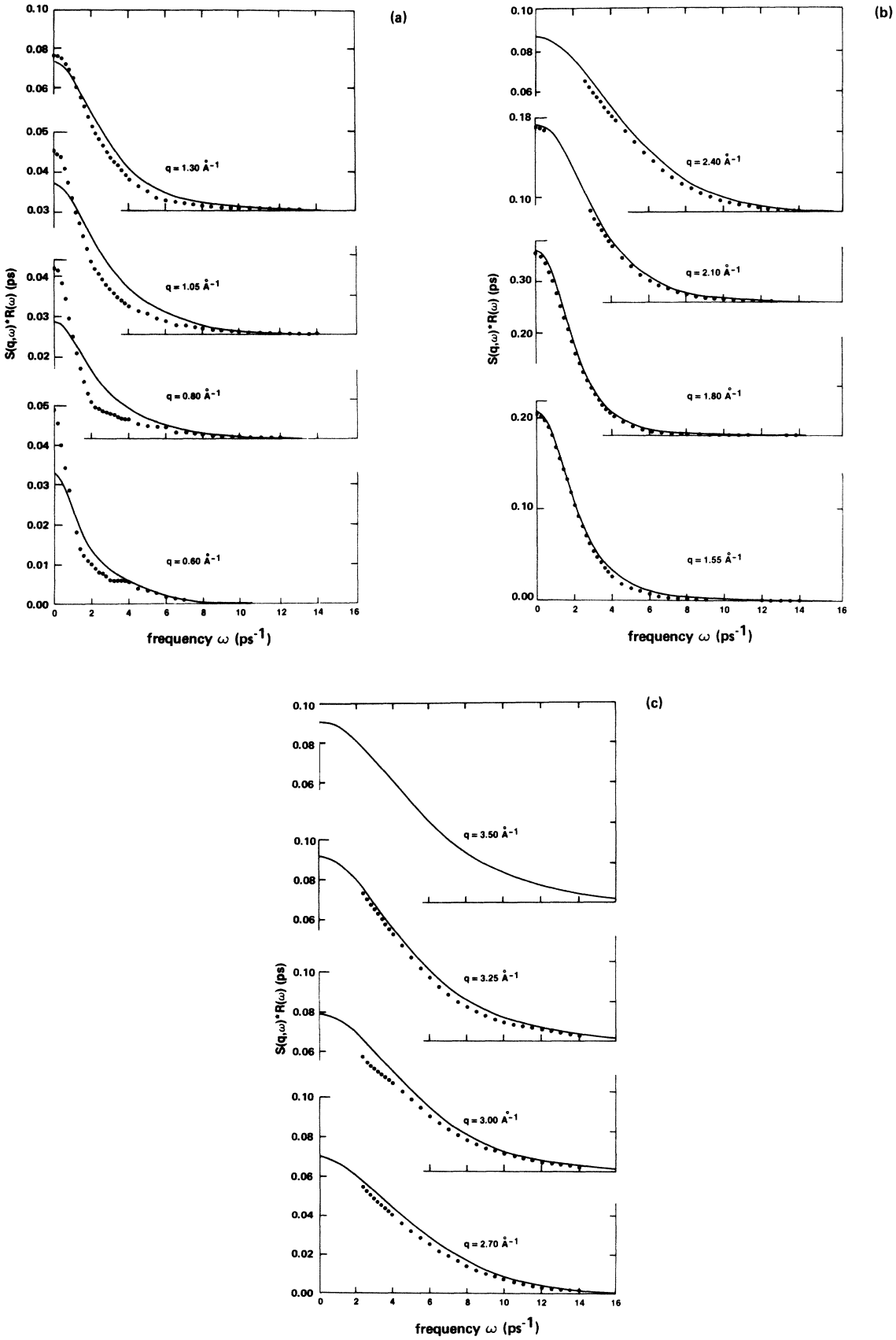

FIG. 4. $S(q,\omega)*R(\omega)$ vs ω for fixed q. The solid line represents an equally weighted average of series I and II results. The dots represent experimental results (Ref. 2). (a) shows results for q of 0.60, 0.80, 1.05, and 1.30 Å^{-1}; (b) 1.55, 1.80, 2.10, and 2.40 Å^{-1}; and (c) 2.70, 3.00, 3.25, and 3.50 Å^{-1}.

tween experiment and simulation is 0.18×10^{-13} sec (5% of peak height) which occurs at $\omega=1.2\times10^{+12}$ sec^{-1}. For the higher q values of 2.40, 2.70, 3.00, and 3.25 Å^{-1} the simulation yields a set of curves which appear to be modestly more intense than the experimental results. Note that for these q values as well as the 2.10 Å^{-1} case, the experimental data has been spoiled by Bragg reflections from the pressure vessel at small ω. The data points in question are omitted so that the comparison with the MD data is incomplete. In the $q=3.50$ Å^{-1} case only the simulation results were obtained.

For curves centered about the origin, the more diffuse or broad a curve is the more sharply peaked or narrow its transform will be. Thus for example, in the $q=1.80$ Å^{-1} case the t space or Fig. 2 curves are quite diffuse while the ω-space transforms are sharply peaked as shown in Fig. 3. In contrast the $q=2.40$ Å^{-1} case shows the t-space curves to be relatively narrow with very diffuse transforms. In the case of the lower q values: $q=1.30$, 1.05, 0.80, and 0.60 Å^{-1}, the simulations produce a curve which is broader than that predicted by the experimental results. This difference between experimental and simulation results becomes more pronounced as q decreases. Hence, the experimentally determined $S(\omega)_*R(\omega)$ will yield an $I(q,t)R(t)$ which is broader than that given by simulation. This in turn suggests that the fluid structures which give rise to the Fourier components $I(q,t)$ for the indicated q values decay more slowly in reality than predicted by our simulation results. Because the differences in Fig. 4 must be due to the failure of the rigid atom approximation, we deduce that the missing many-body terms slow down many-body collision processes at high density (an example of such processes would be ring collisions). Also it is notable that this effect is growing rapidly with density over the range from 10.6—13.8 atoms/nm^3 (i.e., density in Ref. 1 compared to this density).

V. CONCLUSIONS

We have been able to demonstrate that many-body forces significantly affect the dynamics of dense krypton gas. For the state examined in this work, Ram and Egelstaff[14] have shown their contribution to the thermodynamic properties and their effect on the static structure factor was shown by Egelstaff *et al.*[2] However, we have demonstrated for the first time the q and ω dependence of the dynamic-structure factor $S(q,\omega)$ on these forces. In terms of particle dynamics, many-body forces were seen to inhibit the relaxation of longer wavelength fluid structures, i.e., many-body collision processes such as ring collisions are slowed down. It is likely that shorter-ranged polarizability or overlap effects are responsible, partly because of the q range in which the effects are observed and partly because of the consistency of these results with the conclusions of earlier papers discussed in the Introduction.

We have examined the difficulty in obtaining precise molecular dynamics data and further work will involve a better understanding of the errors associated with the simulation of $S(q,\omega)$ and the sensitivity of $S(q,\omega)$ to the pair potential used. However, our comparison of the simulated and experimental $S(q,\omega)$ has been shown to be an effective method of highlighting the importance of many-body forces in dynamic phenomena. Eventually, this may lead to MD simulations using many-body potential functions in order to analyze dynamic phenomena. For example, further simulations using the Axilrod-Teller term and/or overlap terms would be worthwhile.

ACKNOWLEDGMENTS

We would like to thank the Natural Sciences and Engineering Research Council of Canada, GMI Engineering and Management Institute, Flint, Michigan, and the Kernforschungszentrum Karlsruhe, West Germany, for their financial support.

[1]P. A. Egelstaff, J. J. Salacuse, W. Schommers, and J. Ram, Phys. Rev. **30**, 374 (1984).
[2]P. A. Egelstaff, W. Gläser, D. Litchinsky, E. Schneider, and J-B. Suck, Phys. Rev. A **27**, 1106 (1983).
[3]R. A. Aziz, Mol. Phys. **38**, 177 (1979).
[4]J. A. Barker, R. O. Watts, J. K. Lee, T. P. Schafer, and Y. T. Lee, J. Chem. Phys. **61**, 3081 (1974).
[5]F. Barocchi, M. Zoppi, and P. A. Egelstaff, Phys. Rev. A **31**, 2732 (1985).
[6]J. A. Barker, in *Rare Gas Solids*, edited by M. L. Klein and J. A. Venables (Academic, New York, 1976), Vol. 1, Chap. 4, p. 217.
[7]A. Teitsma and P. A. Egelstaff, Phys. Rev. A **21**, 367 (1980).
[8]P. A. Egelstaff, A. Teitsma, and S. S. Wang, Phys. Rev. A **22**, 1702 (1980).
[9]W. Schommers, Phys. Rev. A **22**, 2855 (1980).
[10]W. Schommers, Phys. Rev. A **27**, 2241 (1983).
[11]R. Zwanzig and N. K. Ailawadi, Phys. Rev. **182**, 280 (1969).
[12]P. G. DeGennes, Physica **25**, 825 (1959).
[13]W. Gläser and P. A. Egelstaff (to be published).
[14]J. Ram and P. A. Egelstaff, Phys. Chem. Liq. **14**, 29 (1983).